ISSN 2411-3336; e-ISSN 2541-9404

JOURNAL OF MINING INSTITUTE
Zapiski Gornogo instituta
Journal homepage: pmi.spmi.ru

Research article Geology

The problem of identifying lower crustal garnet-clinopyroxene granulites and mantle eclogites: a case study of xenoliths from the V.Grib pipe

Ekaterina V. Stetskaya[1]✉, **Laysan I. Salimgaraeva**[2], **Aleksei V. Berezin**[2], **Viktor N. Ustinov**[3], **Roman N. Pendelyak**[3]
[1] *Empress Catherine II Saint Petersburg Mining University, Saint Petersburg, Russia*
[2] *Institute of Precambrian Geology and Geochronology RAS, Saint Petersburg, Russia*
[3] *AGD Diamonds JSC, Arkhangelsk, Russia*

***How to cite this article*:** Stetskaya E.V., Salimgaraeva L.I., Berezin A.V., Ustinov V.N., Pendelyak R.N. The problem of identifying lower crustal garnet-clinopyroxene granulites and mantle eclogites: a case study of xenoliths from the V.Grib pipe. Journal of Mining Institute. 2026. Vol. 278, p. 99-114.

Abstract
The article presents a comprehensive analysis of the mineralogical and geochemical features of xenoliths from the V.Grib kimberlite pipe, represented by lower crustal garnet-clinopyroxene granulites and mantle eclogites. A comparative characterization of the two xenolith types is conducted, as clear criteria for their distinction are currently lacking. The study identifies several distinctive features that unequivocally characterize mantle eclogites: elevated Cr contents (in garnets >300 ppm, in clinopyroxenes >1500 ppm), high pyrope content in garnet (>34 mol.%), and evidence of early metasomatism manifested as metasomatic garnet, spongy clinopyroxene replaced by pargasite, and phlogopite rims at garnet-clinopyroxene contacts. Evaluation of the pressure-temperature parameters of the V.Grib pipe xenoliths confirmed the mantle origin of eclogitic xenoliths formed at T = 800-1200 °C and P = 30-50 kbar, and did not refute the initial assumption of a lower crustal origin for granulitic xenoliths characterized by T = 750-800 °C and P = 14-15 kbar. To definitively resolve the issue of identifying lower crustal garnet-clinopyroxene granulites and mantle eclogites, a comprehensive comparison of the isotope-geochemical characteristics of "eclogitic" and "granulitic" zircon is proposed for future research.

Keywords
the V.Grib pipe; *P-T* parameters; lower crustal granulites; mantle eclogites; garnets; clinopyroxenes; xenoliths

Funding
The study was supported by the Russian Science Foundation grant N 24-27-00121.

Received: 16.10.2025 ***Accepted: 24.12.2025*** ***Online: 03.04.2026*** ***Published: 12.05.2026***

Introduction

One of the key methods for studying mantle composition and the deep structure of the Earth's crust is the analysis of xenoliths – fragments of mantle and lower crustal rocks brought to the surface by explosive conduits. Garnet-clinopyroxene rocks are of particular interest, as they can be interpreted as either lower crustal granulites or mantle eclogites. Their reliable identification is of fundamental importance for understanding lithospheric evolution [1], since granulites record lower crustal recycling processes, whereas mantle eclogites provide information on subduction, metasomatism, and recrystallization of mantle material [2, 3].

At present, there is no clear boundary separating eclogite xenoliths from high-pressure lower crustal granulites. Some researchers argue that high-pressure granulites contain distinct mineral assemblages (Grt + Cpx + Pl + Qz), which differ from eclogites by the presence of plagioclase and from medium-pressure granulites by the absence of orthopyroxene [4]. However, other researchers support the less popular theory of a subfacies of plagioclase-bearing eclogites, according to which, in the high-temperature field of the eclogite facies bordering the high-pressure field of the granulite facies,

This is an open access article under the CC BY 4.0 license

© Ekaterina V. Stetskaya, Laysan I. Salimgaraeva, Aleksei V. Berezin, Viktor N. Ustinov, Roman N. Pendelyak, 2026

there exists a field of joint stability for omphacite, garnet, and plagioclase [5-7]. Due to the absence of orthopyroxene in such rock types, equilibrium pressure estimates in deep xenoliths may be biased, as most garnet-clinopyroxene geobarometers are based on equilibrium reactions of these minerals in garnet lherzolites and pyroxenites [8]. The primary criterion for classifying a metamorphic rock as an eclogite is the presence of garnet and high-Na clinopyroxene (omphacite) with a jadeite component exceeding 20 mol.%, and in some cases, specific accessory minerals (kyanite, rutile, coesite) [7].

Nevertheless, in most cases, distinguishing garnet-clinopyroxene deep xenoliths of both types based solely on quantitative mineralogical criteria proves insufficient, necessitating the use of data on the distribution patterns of rare and rare earth elements in rock-forming minerals. The distribution patterns of rare and rare earth elements in minerals represent one of the most informative indicators for refining crystallization conditions, the nature of protoliths, and subsequent metasomatic events. This is well demonstrated in the example of zircon from pegmatites [9] and granites [10].

The problem of classifying garnet-clinopyroxene (Grt-Cpx) xenoliths from the V.Grib kimberlite pipe is particularly relevant, as studies [11-13] have identified zircon in several xenoliths represented by mantle eclogites. Currently, zircon has been confirmed in mantle eclogites from only three kimberlite objects: The Slave craton [14], the V.Grib pipe [11, 12, 15] and the Kasai craton [1, 16], whereas its occurrence in granulite xenoliths is quite common [17, 18].

The aim of this study is a comprehensive analysis of the mineralogical-geochemical features of mantle eclogites and lower crustal garnet (Grt) granulites using xenoliths from the V.Grib pipe, and resolution of their origin (crustal or mantle) through classical thermobarometry methods.

Geological characteristics of the study area

Brief characteristics of the Zimneberezhnyi diamondiferous district (ZBD). Located in the north of the East European Platform, the Zimneberezhnyi district occupies the central part of an uplifted basement block between the Leshuconsk and Keretsko-Pinezhsk Riphean aulacogens. The block consists of crystalline basement overlain by platform deposits of Vendian-Paleozoic and partly Riphean age. The age of the basement and adjacent territories ranges from 2.7 to 1.8 billion years, providing prerequisites for diamondiferous pipes [19]. The territory represents a combination of Archean and Paleoproterozoic granulite-gneiss complexes with Meso- and Cenozoic structures. The Zimneberezhnyi block is likely an Archean structure that did not undergo significant destruction in the Early Proterozoic. The presence of diamondiferous kimberlites indicates preservation of the mantle root [20].

According to A.V.Samsonov and colleagues [19], the Zimneberezhnyi block belongs to the southeastern extension of the Paleoproterozoic Lapland-Kola collisional belt of the Fennoscandian Shield (Fig.1). In the ZBD, seven kimberlite fields of Late Devonian-Early Carboniferous age are distinguished, including two deposits – named after M.V.Lomonosov and V.Grib, which are the most important sources of diamonds for the domestic mineral resource base [21, 22]. Ongoing studies of these deposits form the basis for various model constructions [23-25]. Geochronological studies have shown that the formation of diamondiferous kimberlites occurred in the age interval of 376-378 Ma [26].

Structure of the V.Grib pipe. The V.Grib kimberlite pipe, discovered in 1996, is the most diamondiferous deposit in the East European Province. It is located in the central part of the ZBD, within the Verkhotinsk Uplift of the Ruchievsk Promontory of the crystalline basement. The body, associated with a northeast-trending ore-hosting fault, lies within a local low-contrast structure 2-4 km in diameter (subsidence depression), filled with younger Vendian kimberlite-hosting rocks. The pipe intrudes weakly lithified sedimentary rocks of the Upper Riphean and Upper Vendian and is overlain by a thickness of terrigenous and carbonate rocks of the Middle Carboniferous and loose

This is an open access article under the CC BY 4.0 license

© Ekaterina V. Stetskaya, Laysan I. Salimgaraeva, Aleksei V. Berezin, Viktor N. Ustinov, Roman N. Pendelyak, 2026

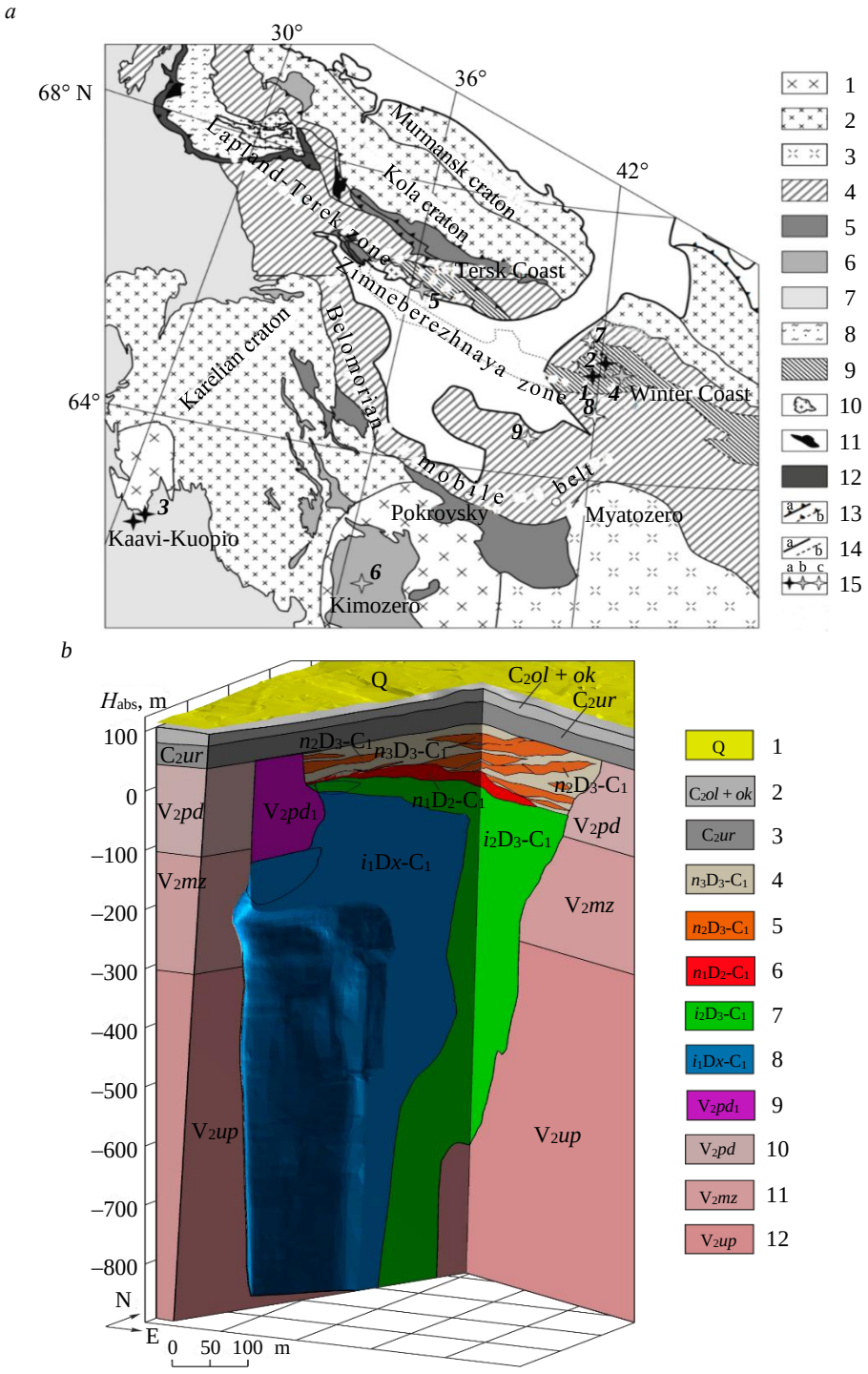


Fig.1. North of the East European Platform:
a – Tectonic scheme [19]: 1-3 – Archean blocks: 1 – Mesoarchean, 2 – Neoarchean, 3 – of undetermined age; 4 – Belomorian mobile belt; 5-12 – Paleoproterozoic structures: 5 – 2.45 Ga, 6 – 2.45–1.75 Ga, 7 – 2.0-1.7 Ga; 8-12 – Lapland-Tersky and Zimneberezhnaya suture zones: 8 – metasediments, 9 – TTG orthogneisses, granitoids, 10 – enderbites, charnockites, 11 – anorthosites, 12 – collision mélange; 13, 14 – tectonic discontinuities: 13 – thrusts (a – established, b – inferred), 14 – others: a – established, b – inferred; 15 – manifestations (fields) of kimberlite and related magmatism: a – diamondiferous (*1* – Zolotitskoye, *2* – the V.Grib pipe, *3* – Kaavi-Kuopio), b – poorly diamondiferous (*4* – Kepinskoye, *5* – Ermakovskaya pipe, *6* – Kimozero), c – non-diamondiferous (*7* – Melskoe, *8* – Chidvinsko-Izhmozero, *9* – Nenokskoye);
b – 3D model of the V.Grib pipe [20]: 1-3 – deposits overlying the kimberlite pipe: 1 – Quaternary, 2 – Olmug-Okunevskaya Formation, 3 – combined Urzuga and Voerechenskaya Formations; 4-6 – rocks of the crater facies: 4 – sandstones and tuff sandstones, 5 – tuff sandstones, tuffites, and tuffs, 6 – tuffs, tuffites; 7, 8 – rocks of the vent facies (intrusion sequence): 7 – autolithic kimberlite breccia and porphyritic kimberlite (final), 8 – xenotuff breccia and tuff breccia (initial); 9 – zone of disintegrated sandstones; 10-12 – host rocks of the Late Proterozoic kimberlite-hosting basement, Upper Vendian Formation: 10 – Padunskaya, 11 – Mezenskaya, 12 – Ust-Pinezhskaya

This is an open access article under the CC BY 4.0 license

Quaternary deposits (Fig.1, *b*). On the buried surface, the pipe has a rhomboid-rounded shape in plan (575×500 m), elongated in the northeast direction, with an area at the erosion level of 16 ha. At depths of 800-1000 m, the pipe transitions into an asymmetric dyke-like body of similar orientation.

The V.Grib pipe has a complex structure with two main intrusion phases distinguished by mineral composition, textural features, and diamond potential – xenotuff breccias and kimberlites [20]. Tuff- and xenotuff breccias formed first, followed by autolithic kimberlite breccias and porphyritic kimberlites. The tuff- and xenotuff breccias are subdivided into two phases, while the autolithic kimberlite breccias and porphyritic kimberlites are presumably divided into four phases. This structure indicates multiple kimberlite magma intrusions and a pulsatory nature of magmatic activity, consistent with modern models of primary diamond deposit formation [27]. Recent studies of diamonds from the V.Grib pipe kimberlites [28] have established a high proportion of low-nitrogen crystals and individuals with Ni impurities, which may be indicators of large CLIPPIR-type crystals in the deposit. This points to specific crystallization conditions distinct from those of other kimberlite bodies in the East European, Siberian Platforms and Ural placers.

Deep-seated xenoliths of the V.Grib pipe. Mantle xenoliths from the V.Grib kimberlite pipe are represented by a wide spectrum of deep-seated ultramafic rock compositions: spinel and garnet peridotites (lherzolites and harzburgites), pyroxenites (websterites), and eclogites, studied in detail over several years [29]. In turn, lower crustal xenoliths from this pipe remain insufficiently studied [17, 18] and are classified as Grt-Cpx granulites or Grt-clinopyroxene (eclogite-like) rocks.

For this study, six samples of garnet-clinopyroxene xenoliths from the V.Grib pipe, provided by AGD Diamonds JSC, were selected as rock material.

Methods

Analysis of chemical composition of the studied xenoliths. Due to the severe limitation of the rock material, the analysis was performed not for six, but for five samples. The contents of major elements were analyzed by X-ray fluorescence spectroscopy (XRF) on a multichannel ARL-9800 spectrometer using a standard procedure (Karpinsky Institute). The lower detection limits for petrogenic element oxides are 0.01-0.05 wt.%. The contents of trace and rare earth elements (REE) were determined by inductively coupled plasma mass spectrometry (ICP-MS) on a quadrupole ELAN-DRC-6100 mass spectrometer using a standard procedure (Karpinsky Institute) with acid decomposition in a mixture of acids (HF + HNO_3). Geological USGS standards were used to control analysis accuracy. The relative error of determination for more than 70 elements does not exceed 5-10 % – for REE less than 5 %, for Rb, Sr, Ba, Nb, Ta, Zr, Hf, U, and Th – less than 10 %. Lower detection limits range from 0.01 % for major elements and 0.005-0.010 ppm for most trace and rare earth elements.

Chemical composition of minerals. The composition of minerals, as well as features of their structure and interrelationships, were studied in epoxy resin thin sections (polished mounts) in backscattered electron (BSE) mode on a JEOL JSM-6510LA scanning electron microscope equipped with an energy-dispersive spectrometer JED-2200 (IPGG RAS). Mineral end-member compositions were calculated using the Minal 3.0 program developed by D.V.Dolivo-Dobrovolsky (IPGG RAS) [30], empirical mineral formulas were calculated in accordance with the recommendations of V.G.Krivovichev and Yu.L.Gulbin [31]. Amphibole compositions were calculated based on the recommendations and classification scheme approved by the IMA [32]. Mineral abbreviations are given according to article [33].

The contents of trace elements in minerals were determined by secondary ion mass spectrometry (SIMS) on a Cameca IMS-4f ion microprobe at the Valiev IPT RAS, Yaroslav branch. The measurement error for trace elements is up to 10 % for concentrations above 1 ppm and up to 20 % for the concentration range 0.1-1 ppm; the detection threshold for various elements varies within 5-10 ppb. The trace element composition of rock-forming minerals was determined in the same

This is an open access article under the CC BY 4.0 license

© Ekaterina V. Stetskaya, Laysan I. Salimgaraeva, Aleksei V. Berezin, Viktor N. Ustinov, Roman N. Pendelyak, 2026

areas as the major element analyses. For constructing REE distribution patterns, mineral compositions were normalized to CI chondrite composition [34]. Eu- and Ce-anomaly values were calculated

$$Eu/Eu^* = EuN/\sqrt{(SmN)(GdN)};$$

$$Ce/Ce^* = CeN/\sqrt{(LaN)(PrN)}.$$

Methodology for selecting geothermometers and geobarometers. In this study, the methodology is determined by the bimineralic nature of the studied samples. *P-T* parameters of eclogitic xenoliths were estimated using four geothermometers based on Fe-Mg exchange between garnet and omphacite – EG79, P85, A94 [35-37] and K00 [38], each calibrated to a geotherm with a value of 40 mW/m^2, as nearly all modern estimates of heat flow beneath Archean cratons are on the order of 38-42 mW/m^2 [39]. An empirical Grt-Cpx barometer designed for mantle eclogites – BFM15 – was used [40]. For determining *P-T* parameters of lower crustal high-pressure granulites, the same Grt-Cpx geothermometers (EG79, P85, A94, K00) as for eclogites were applied, but pressure was determined "directly" using the Pl-Cpx-Grt-Qtz geobarometer NP82 [41]. Additionally, the Ti-in-zircon thermometer (Ti-in-Zrn) was used to determine granulite-facies metamorphism temperature [42]. Attempts to apply the BFM15 geobarometer were unsuccessful – the method yielded anomalously low pressures <5 kbar, so it had to be excluded.

Results

Petrographic characteristics. Eclogite xenoliths (samples 334-137, 8-25-100, 11-30-11) are represented by dark green rocks with massive texture and medium-grained granoblastic structure (Fig.2, *a*). The rock-forming minerals of the xenoliths are hypidiomorphic garnet and strongly opacitized clinopyroxene, occupying 80 to 90 % of the rock volume. Garnet in all samples is represented by large rounded grains 0.3-1.5 cm in size with strong fracturing and is situated in a matrix of large clinopyroxenes up to 0.5 cm. It is noteworthy that xenoliths of this type are characterized by the presence of phlogopite rims up to 1 mm at the contacts of garnet and clinopyroxene grains, as well as serpentine veinlets cutting them. No inclusions were found in garnet and clinopyroxene, but both minerals are strongly altered.

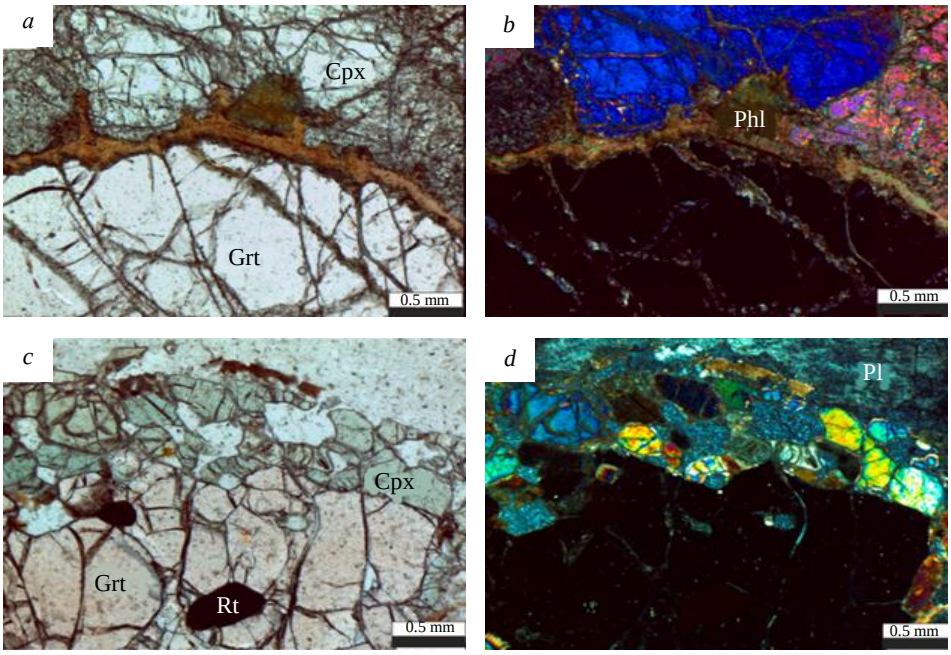


Fig.2. Photomicrographs of thin sections: *a*, *b* – mantle eclogite (sample 11-30-11); *c*, *d* – garnet-clinopyroxene granulite (sample 252-30); *a*, *c* – without analyzer; *b*, *d* – with analyzer

This is an open access article under the CC BY 4.0 license

Granulite xenoliths (samples 252-30, 272-112, 335-137) are characterized by medium-grained granoblastic structure with massive (sample 335-137) and banded texture (samples 272-112, 252-30), where banding is formed by leucocratic and melanocratic zones 0.2-0.5 cm wide. Melanocratic zones consist of hypidiomorphic garnet up to 1 cm and xenomorphic clinopyroxene 0.2-0.5 mm, sometimes occurring as inclusions in garnet in the samples (272-112, 335-137) (Fig.2, *b*). Scales of phlogopite up to 0.2 mm oriented along the banding direction are observed in samples 272-112 and 252-30 and are more closely associated with clinopyroxene. Leucocratic zones are composed of acid plagioclase, sometimes almost completely replaced by potassium feldspar, and a serpentine-chlorite cryptocrystalline mass (up to 30 % of the rock volume). Garnet grains (less commonly clinopyroxene) contain diverse inclusions represented by quartz (~0.025 mm), unaltered rutile, and apatite.

The bulk composition of the rocks was determined for three Grt-Cpx granulite samples (252-30, 272-112, 335-137) and two eclogite samples (334-137, 8-25-100). Unfortunately, due to the small size of the xenolith, it was impossible to analyze the bulk composition of sample 11-30-11.

Major elements. All xenoliths correspond to monzogabbro in terms of compositional features, except for sample 334-137 (this eclogite plots in the gabbro field). Grt granulites are characterized by elevated $Na_2O + K_2O$ content and reduced MgO and FeO relative to eclogites (Table 1).

Table 1

The results of XRF chemical analysis of the studied rocks, wt.%

Sample	Major Element Oxides										LOI*	Total
	SiO_2	Al_2O_3	TiO_2	Fe_2O_{3tot}	MnO	MgO	CaO	Na_2O	K_2O	P_2O_5		
8-25-100	40.1	14.0	0.33	8.77	0.21	15.3	6.34	2.06	1.19	0.55	11.1	100.0
334-137	45.5	14.0	0.95	9.40	0.32	18.6	2.55	0.38	2.68	0.12	3.71	98.1
252-30	43.5	15.2	1.00	9.15	0.09	15.4	2.52	1.42	2.65	0.13	7.18	98.3
272-112	44.4	14.9	0.82	9.76	0.17	12.8	8.42	1.65	2.74	0.25	3.37	99.3
335-137	45.2	17.3	1.68	15.3	0.28	6.80	8.23	2.20	1.43	0.71	0.50	99.6
Limits of detection	0.02	0.05	0.01	0.01	0.01	0.1	0.01	0.1	0.01	0.05	–	–

* LOI – loss on ignition.

Trace elements. REE spectra for all studied rocks exhibit a differentiated pattern with depleted HREE relative to LREE. Granulites show a distinct positive Eu anomaly (Eu/Eu* ~1.42), which may be due to the presence of plagioclase. No clear pattern in REE distribution at the rock level is observed between eclogites and granulites (Fig.3). Regarding trace elements, granulite xenoliths relative to eclogites are characterized by elevated Ba and Sr values, which also positively correlate with plagioclase content, and depleted Cr and Cu (Table 2). No clear pattern is observed for the other trace elements.

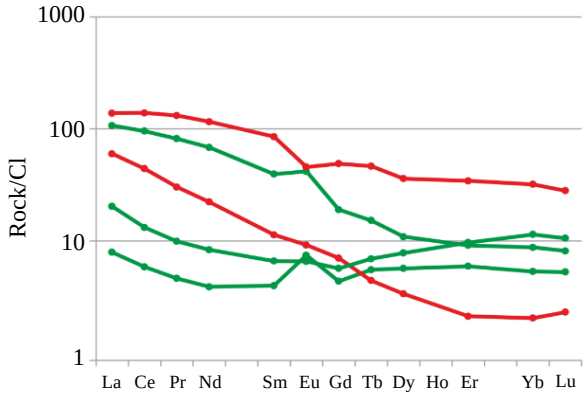


Fig.3. REE distribution patterns in xenoliths
Green – granulites; red – eclogites;
REE contents normalized to CI chondrite composition [35]

Rock-forming minerals. Garnet from the studied xenoliths belongs to the almandine-grossular-pyrope series. Garnets from granulites and eclogites have their structural differences. Eclogite garnets are characterized by phlogopite rims forming at contacts with clinopyroxene (Fig.4, *a*), whereas granulite garnets contain inclusions of apatite, rutile, quartz, and sometimes clinopyroxene (Fig.4, *c*, *d*).

This is an open access article under the CC BY 4.0 license

© Ekaterina V. Stetskaya, Laysan I. Salimgaraeva, Aleksei V. Berezin, Viktor N. Ustinov, Roman N. Pendelyak, 2026

Table 2

Chemical compositions of the studied rocks based on ICP-MS results, ppm

Trace elements	Sample					Limits of detection
	272-112	334-137	252-30	335-137	8-25-100	
Sc	17.8	7.15	18.6	59.2	28	0.2
V	98.8	94.5	179	202	257	2.5
Cr	711	86.6	308	10,120	134	1
Co	50.1	26.4	37.7	54.7	31.5	0.5
Ni	238	93	173	661	84.7	1
Cu	15.7	5.17	20.1	108	44.5	1
Zn	37.3	67.9	86.7	24.6	103	1
Ga	4.67	11.1	14.8	8.35	20.6	0.1
Rb	4.54	32.4	20	16.9	12	2
Sr	374	782	841	79.4	589	1
Y	8.88	4.02	14.4	12.4	53	0.1
Zr	11.4	227	58.8	25.1	172	0.5
Nb	3.65	7.76	8.87	5.05	14.6	0.5
Ba	1490	16,730	6550	170	1890	3
La	1.88	14.2	25.4	4.82	32.7	0.01
Ce	3.60	27.1	58.5	8.08	85	0.01
Pr	0.43	2.81	7.58	0.92	12.2	0.01
Nd	1.78	10.2	31.2	3.81	52.9	0.01
Sm	0.59	1.68	5.84	0.98	12.6	0.005
Eu	0.42	2.85	2.35	0.37	2.57	0.005
Gd	0.87	1.40	3.79	1.13	9.74	0.01
Tb	0.20	0.16	0.55	0.25	1.68	0.005
Dy	1.40	0.83	2.68	1.92	8.86	0.01
Ho	0.32	0.15	0.50	0.48	1.95	0.005
Er	0.95	0.34	1.46	1.55	5.49	0.01
Tm	0.14	0.053	0.21	0.25	0.80	0.005
Yb	0.86	0.33	1.41	1.84	5.15	0.01
Lu	0.13	0.057	0.20	0.26	0.69	0.005
Hf	0.36	6.17	2.02	0.90	4.83	0.01
Ta	<0.1	0.40	0.45	0.24	0.55	0.1

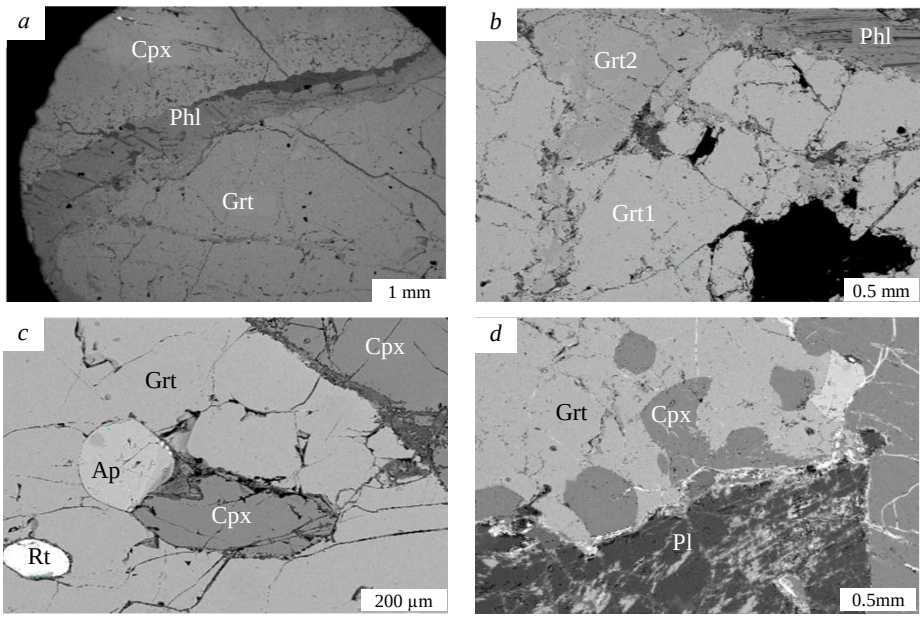


Fig.4. Garnet in eclogites (*a*, *b*) and granulites (*c*, *d*) in back-scattered electron (BSE) image

This is an open access article under the CC BY 4.0 license

Major elements. Chemical zoning in eclogite garnets is weakly expressed. In all three samples, a slight decrease in pyrope (Prp) and increase in almandine (Alm) components is observed from center to rim. In sample 8-25-100, a later generation of metasomatic garnet was identified, developing from grain edges along cracks in the primary mineral and manifesting extremely unevenly (Fig.4, *b*). The newly formed garnet differs from the primary one by higher magnesian content – #Mg of metasomatic garnet exceeds #Mg of the unaltered central part by approximately 1.3 times (Supplement 1, https://pmi.spmi.ru/pmi/article/download/16832/16630). Metasomatic garnet is also characterized by high TiO_2 content up to 0.73 wt.% and low CaO ~8.37 wt.% compared to the primary mineral. Garnets from granulites have a more homogeneous composition, but samples 252-30 and 335-137 also show weakly expressed reverse zoning.

According to the mineral composition diagram (Fig.5, *a*), eclogite garnets differ by high Prp content compared to granulite garnets, though some features exist. Garnets from samples 11-30-11 and 334-137, containing Cr_2O_3 admixture (up to 3 wt.% in unaltered central parts), are unambiguously pyropes (Prp_{67-69}, Alm_{17-24}, Grs_{1-8}), whereas garnets from sample 8-25-100 have roughly equal amounts of all three components – Prp_{34-35}, Alm_{36}, Grs_{27} in primary garnet and Prp_{53}, Alm_{30}, Grs_{16} in metasomatic. Garnets from samples 252-30, 272-112, 335-137, representing lower crustal granulites, belong to the pyrope-almandine series (see Table 1) and are characterized by the following end-member composition – Prp_{24-36}, Alm_{47-53}, Grs_{15-21} (Supplement 1, https://pmi.spmi.ru/pmi/article/download/16832/16630).

Trace elements. In most garnets from the studied xenoliths, REE distribution spectra preserve a general pattern – sharp differentiation from LREE to HREE with enrichment in heavy REE (Fig.5, *b*). The normal REE distribution type typical for mantle eclogite garnets is characteristic of all samples except sample 252-30, a granulite. Garnet from this xenolith has anomalously low HREE content

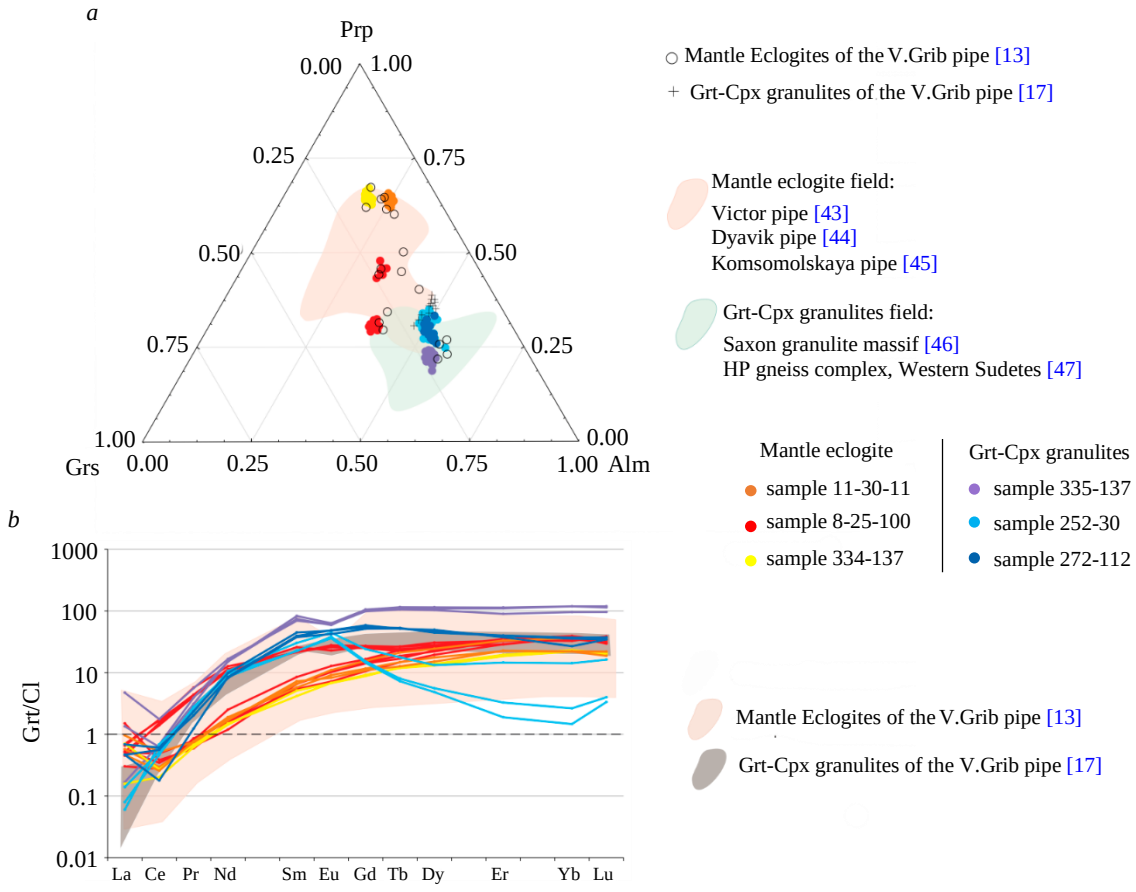


Fig.5. Comparative diagram of garnet end-member compositions (*a*); REE distribution spectra in garnets (*b*)
REE contents are normalized to the CI chondrite composition [34]

This is an open access article under the CC BY 4.0 license

and a peculiar sinusoidal spectrum (Fig.5, *b*), with rim parts more depleted in HREE compared to centers. In the other xenoliths, no pronounced heterogeneity in REE distribution is observed. Granulite sample 335-137 stands out by elevated REE content (∑REE = 120 ppm), while the lowest is in sample 11-30-11, a mantle eclogite (∑REE = 18.4 ppm) (Supplement 2, https://pmi.spmi.ru/pmi/article/download/16832/16631). Note that most REE spectra in garnets from eclogites and granulites fall within the field of garnets from V.Grib pipe mantle eclogites described earlier [13] (Fig.5, *b*).

Trace element distribution in garnets (Table 2) shows elevated Cr content in mantle eclogites compared to lower crustal granulites (>300 ppm in grain centers) (see Supplement 1, https://pmi.spmi.ru/pmi/article/download/16832/16630). Contents of other elements in eclogite and granulite garnets are in approximately the same range.

Clinopyroxene in eclogites forms micro- to fine-grained aggregates with high porosity of spongy appearance in rim zones, replaced by amphibole of predominantly pargasitic composition in interstices (Fig.6, *a*, *b*). Clinopyroxenes from garnet granulites are characterized by homogeneous structure (Fig.6, *c*).

Major elements. Clinopyroxenes from most eclogite xenoliths contain Cr_2O_3 admixture (up to 1 wt.% in unaltered central parts), negatively correlating with Na_2O (up to 2 wt.% in unaltered central parts). Altered clinopyroxene with spongy structure differs from central parts by elevated FeO, MgO, CaO and reduced Na_2O (Supplement 3, https://pmi.spmi.ru/pmi/article/download/16832/16632). The composition of unaltered central parts of clinopyroxene in eclogites and granulites contains more Na compared to inclusions in garnet and rims (Jd end-member difference up to 2 %).

According to the classification of L.Taylor and C.Neal [48], based on MgO and Na_2O contents in clinopyroxenes distinguishing mantle eclogite groups *A*, *B*, and *C*, the studied samples belong to groups *A* and *B* (Fig.7, *b*). Per this classification, group *A* eclogites represent cumulates of mantle melts; group *B* eclogites – restites of oceanic crust basalt melting; group *C* eclogites – restites of plagioclase-enriched oceanic crust melting. On this diagram, it is evident that the chemical composition of clinopyroxenes from lower crustal granulites (samples 252-30, 272-112, 335-137) shows considerable similarity to the theoretical composition of clinopyroxenes from group *B* mantle eclogites; Cr-bearing clinopyroxenes from mantle eclogites (11-30-11, 334-137) plot in group *A* (Fig.7, *b*). One eclogite xenolith occupies an intermediate field between groups (8-25-100)

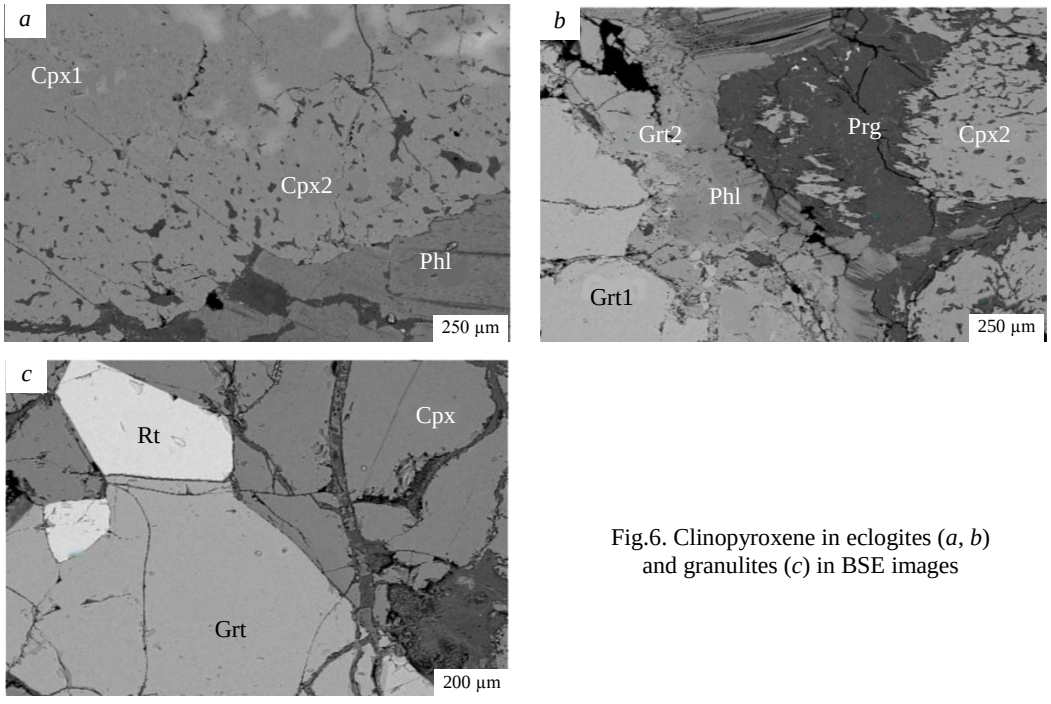


Fig.6. Clinopyroxene in eclogites (*a*, *b*) and granulites (*c*) in BSE images

This is an open access article under the CC BY 4.0 license

© Ekaterina V. Stetskaya, Laysan I. Salimgaraeva, Aleksei V. Berezin, Viktor N. Ustinov, Roman N. Pendelyak, 2026

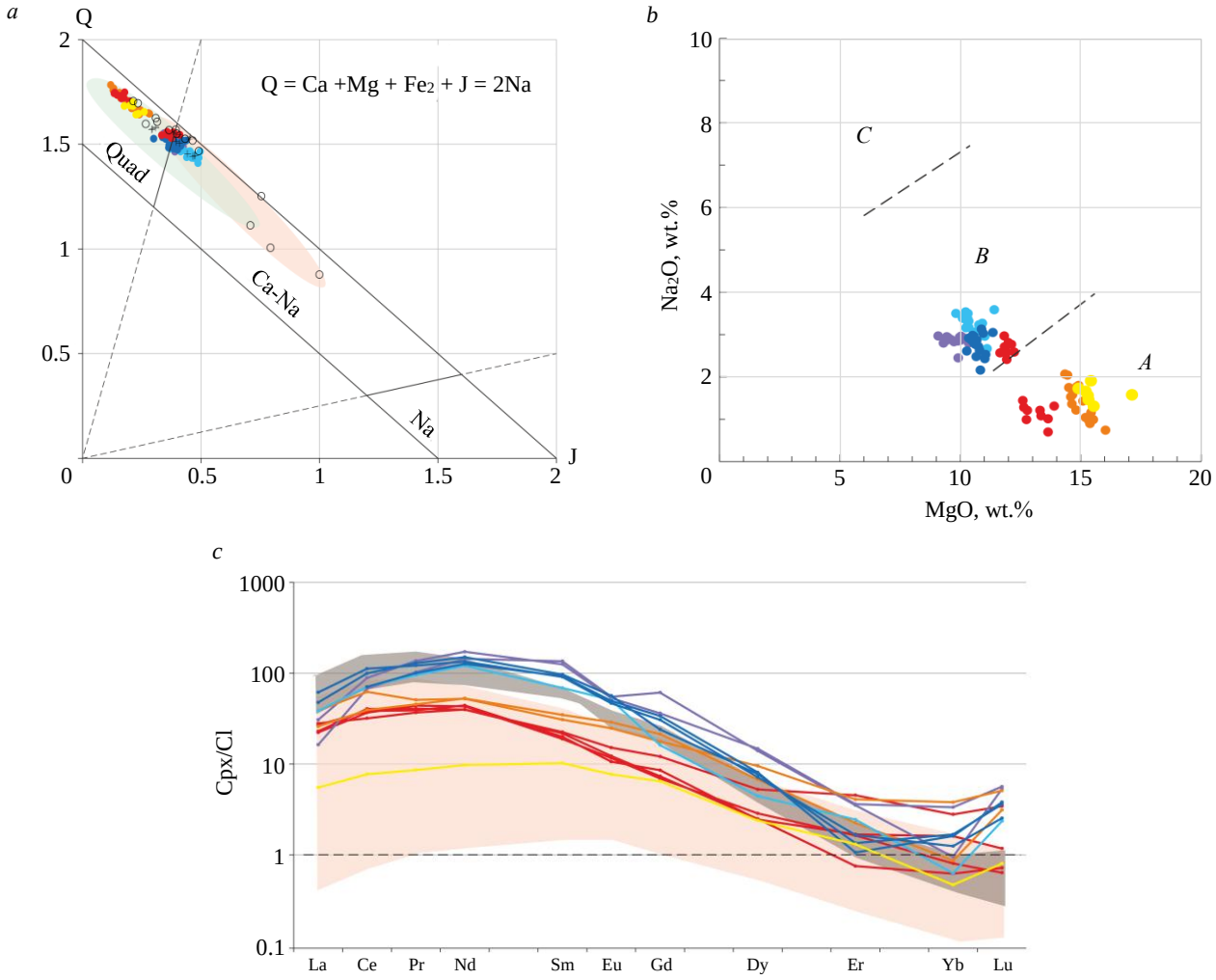


Fig.7. Classification diagrams for clinopyroxenes: *a* – after N.Morimoto [49]; *b* – after L.Taylor and C.Neal [48]; *c* – REE distribution spectra

REE contents are normalized to the CI chondrite composition after W.McDonough [34]. Symbol explanations are given in Fig.5

due to abundant altered clinopyroxene in the sample (up to 40 vol.%), which has reduced Na_2O contents. Unaltered central parts of clinopyroxene from this eclogite plot in group *B*.

According to the classification of N.Morimoto et al. [49] (Fig.7, *a*), clinopyroxenes from eclogite xenoliths have low jadeite end-member content and belong to diopside.

Trace elements. REE content in clinopyroxenes from the studied xenoliths is characterized by a differentiated spectrum with a decrease from LREE to HREE (Fig.7, *c*).

Clinopyroxenes from garnet granulites differ from eclogites by ~2.5 times higher total REE (see Supplement 2, https://pmi.spmi.ru/pmi/article/download/16832/16631), but the REE distribution pattern is the same in both types.

Plagioclase. Partially replaced plagioclase grains in leucocratic zones of banded garnet granulites are mostly oligoclase An_{15-18} Ab_{79-82} Or_{2-5} (Supplement 4, https://pmi.spmi.ru/pmi/article/download/16832/16633).

Secondary minerals. *Phlogopite.* Micas in all studied xenoliths are classified as phlogopites (Supplement 4, https://pmi.spmi.ru/pmi/article/download/16832/16633). In eclogite xenoliths, this mineral occurs as rims at contacts of rock-forming minerals, whereas in garnet granulites, phlogopite is unevenly distributed and oriented along the banding direction of samples. A distinctive feature of chemical composition is the higher magnesian content of eclogite phlogopite (~85 %) compared to granulite phlogopite (~75 %).

This is an open access article under the CC BY 4.0 license

Amphiboles develop in eclogites in paragenetic zones of rock-forming minerals, replacing spongy altered clinopyroxene. According to the classification in [50], amphiboles are pargasites. Their composition varies depending on the degree of amphibolitization – in the most amphibolitized sample 334-137, magnesian content is almost twice that in weakly amphibolitized sample 8-25-100 (Supplement 4, https://pmi.spmi.ru/pmi/article/download/16832/16633).

P-T conditions. Estimates of pressure and temperature of mantle eclogite xenolith formation were made using average compositions of central unaltered zones of garnets and clinopyroxenes obtained from several points in different grains, as mineral contact zones in these samples are represented by metasomatic garnet and spongy clinopyroxene reflecting later conditions. This method is due to the homogeneity of central parts of garnet and clinopyroxene grains and is popular in mantle eclogite studies, as such xenoliths are often strongly altered.

In garnets of all three granulite xenoliths, single quartz inclusions ~25 μm in size lack radial cracks formed during coesite-quartz transition. This imposes constraints on the pressure values at which inclusions were captured, making estimation of this parameter using the heat flow geotherm impossible. The lack of distinct chemical and structural-textural zoning in rock-forming minerals from Grt granulites allows concluding equilibrium of this mineral system. Therefore, for determining formation conditions of such xenoliths, analyses of grain rims, where possible in mutual contact, were used.

Zircon crystallization temperatures from Grt-Cpx granulites (samples 252-30, 272-112) range from 724 to 789 °C (Table 3). For *P-T* parameter calculations of granulite formation, the average temperature for zircon rims and its partially recrystallized core was used. Calculations of formation temperatures for mantle eclogite xenoliths using various Grt-Cpx geothermometer calibrations yield results differing by nearly 100 °C. Pressure values calculated using the heat flow geotherm (40 mW/m^2) and Grt-Cpx barometer [40] have an average error of 10 kbar. Temperature calculations for Grt granulites using all five geothermometers show similar scatter – in some cases, the difference exceeds 150 °C (largest for K00 and EG79 geothermometers).

Table 3

Calculated *P-T* parameters of the xenolith formation conditions

Rock	Sample	Geothermometers					Geobarometers
		K00 (±30 °C)	P85 (±30-40 °C)	A94 (±70 °C)	EG79 (±50 °C)	Ti-in-Zrn (±10-20 °C)	
Eclogites	8-25-100	1175 °C 45 kbar	1050 °C 43 kbar	1080 °C 45 kbar	1040 °C 43 kbar		40 mW/m^2
		1180 °C 53 kbar	1080 °C 54 kbar	1150 °C 58 kbar	1075 °C 52 kbar		BFM15
	11-30-11	925 °C 38 kbar	1000 °C 44 kbar	800 °C 30 kbar	950 °C 39 kbar		40 mW/m^2
		950 °C 43 kbar	1050 °C 50 kbar	925 °C 47 kbar	1000 °C 48 kbar		BFM15
	334-137	990 °C 40 kbar	1010 °C 43 kbar	1200 °C 53 kbar	1175 °C 51 kbar		40 mW/m^2
		1050 °C 51 kbar	1045 °C 50 kbar	1300 °C 63 kbar	1200 °C 58 kbar		BFM15 (±1-2 kbar)
Granulites	335-137	740 °C 14 kbar	750 °C 15 kbar	795 °C 15 kbar	870 °C 17 kbar		NP85 (±1-3 kbar)
	252-30	700 °C 13 kbar	720 °C 14 kbar	750 °C 14 kbar	850 °C 15 kbar	742 °C	
	272-112	710 °C 13 kbar	735 °C 14 kbar	770 °C 15 kbar	820 °C 15 kbar	760 °C	

This is an open access article under the CC BY 4.0 license

© Ekaterina V. Stetskaya, Laysan I. Salimgaraeva, Aleksei V. Berezin, Viktor N. Ustinov, Roman N. Pendelyak, 2026

Discussion

Petrographic examination of six deep-seated xenoliths from the V.Grib kimberlite pipe revealed two rock varieties distinguished by structural-textural features and mineral assemblages – eclogites and Grt-Cpx granulites. All xenoliths correspond to monzogabbro and gabbro in composition, with no clear pattern in the distribution of REE and trace elements observed at the whole-rock level between eclogites and granulites. Garnets from the studied xenoliths belong to the almandine-grossular-pyrope series. Chemical zonation in garnets from eclogites is weakly expressed. In most samples, a slight decrease in Prp and increase in Alm contents from core to rim is observed, representing reverse zonation as a result of exhumation of the eclogite xenolith during ascent of the host kimberlite [51]. In eclogite sample 8-25-100, a later generation of metasomatic garnet was identified, developing from grain margins along cracks and differing from the primary garnet by elevated magnesian content, whereas garnets from granulite xenoliths exhibit a more homogeneous composition. Metasomatic garnet in mantle eclogite xenoliths with similar structural-geochemical features has been described in works by N.M.Lebedeva et al. [52] and D.S.Mikhailenko et al. [53], interpreted as the result of "…early metasomatism under the influence of carbonate-ultramafic melts" [52]. Garnets from eclogites are enriched in the pyrope component – Prp_{34-69} Alm_{17-36} Grs_{8-27} – compared to those from granulites – Prp_{24-36} Alm_{47-53} Grs_{15-21}. Nearly all garnets from the studied samples (except granulite specimen 335-137) plot in the field of "classical" mantle eclogites from Canada and Yakutia [44, 45, 50], while compositions of mantle eclogite garnets from the V.Grib pipe described by predecessors [13], fully overlap with garnets from both types of xenoliths we are considering – both granulites and eclogites (see Fig.5). However, when comparing garnet compositions from our xenoliths with those from lower crustal granulites of high-grade metamorphic complexes in Eastern Germany and the Western Sudetes [46, 47] garnets from Grt-Cpx granulites of the V.Grib pipe occupy an overlapping zone between "granulite" and "eclogite" garnet fields (see Fig.5, *a*).

Clinopyroxenes from eclogites are often altered at margins with a spongy texture and development of pargasite. Formation of such spongy structures in clinopyroxene has been noted in many mantle eclogites by various researchers and interpreted as "…the result of combined decompression during kimberlite ascent and fluid flow infiltrating xenoliths along cracks" [54]. Altered zones in eclogite clinopyroxenes are characterized by reduced Jd content (down to 6 mol.%) compared to grain cores (up to 19 mol.%), whereas granulite clinopyroxenes show elevated Jd (around 20 mol.%). Na_2O loss in clinopyroxene may be interpreted as a result of intense metasomatic processes, evidenced by abundant phlogopite rims around garnet and the spongy appearance of clinopyroxene. However, most plotted clinopyroxene compositions from mantle eclogites of the V.Grib pipe described earlier [13], also feature low Na_2O (average Jd < 20 mol.%) (Fig.7, *a*). The widely used classification of mantle eclogites by L.Taylor and C.Neal proved unsuitable for distinguishing lower crustal granulites from eclogites, as clinopyroxenes from lower crustal granulites fall into the Group *B* mantle eclogite field (Fig.7, *b*).

Thus, it can be concluded that it is impossible to correctly distinguish lower crustal Grt-Cpx granulites from mantle eclogites at the level of major-element compositions of rock-forming minerals. Features distinguishing mantle eclogites include high pyrope content in garnet (>34 %), signs of metasomatic processes (metasomatic garnet, spongy clinopyroxene with pargasite, phlogopite rims at garnet-clinopyroxene contacts), and absence of plagioclase interlayers in the rock.

Most garnets from the studied xenoliths show sharp LREE/HREE fractionation with enrichment in HREE. The exception is granulite garnet from specimen 252-30 with anomalously low HREE content. Such an inflection in the HREE region in garnet likely resulted

This is an open access article under the CC BY 4.0 license

from mineral interaction during coeval growth with fine-dispersed REE phosphates, e.g., monazite [55]. REE contents in clinopyroxenes exhibit fractionated patterns decreasing from LREE to HREE, explained by the presence of garnet – a typical HREE concentrator – in the paragenesis.

Comparative analysis of REE and trace element distribution in rock-forming minerals of granulites and eclogites revealed nearly identical REE patterns in garnet and clinopyroxene of both xenolith types, with minor differences in trace element composition (eclogite minerals show elevated Cr, in garnets >300 ppm, in clinopyroxenes >1500 ppm), interpretable as a criterion of greater depth [56].

Notably, previously described zircon-bearing mantle eclogites [13], show strong similarity in structural-textural features, rock-forming mineral compositions (low Prp in garnet with high Jd in clinopyroxene), and REE distribution to lower crustal Grt-Cpx granulites.

In interpreting classical thermobarometry results, crystallization of zircon rims and recrystallization of its magmatic cores likely occurred during granulite-facies metamorphism, with the Ti-in-Zrn geothermometer providing the most adequate temperature estimate. Among classical geothermometers, A94 is most reliable [37], as its results are closest to Ti-in-Zrn [42] (Table 3). For consistent *P-T* comparison of xenolith formation conditions, eclogite temperatures should be estimated using the same geothermometer.

Eclogite xenolith formation temperatures range from 800 to 1200 °C at 30-50 kbar, confirming their mantle origin. Grt granulite formation temperatures are 750-800 °C at 14-15 kbar, consistent with lower crustal origin. Garnet-clinopyroxene granulites belong to the transition between eclogite and granulite facies [4]. Temperatures for previously studied zircon-bearing mantle eclogites (740-810 °C by K00 and 810-870 °C by EG79) [13], are close to those for lower crustal granulites considered here.

Conclusion

This study conducted a comprehensive petrological, geochemical, and thermobarometric investigation of xenoliths from the V.Grib kimberlite pipe. Two types of xenoliths were distinguished: mantle eclogites and lower crustal Grt-Cpx granulites.

It is suggested that only elevated Cr contents (in garnets >300 ppm, in clinopyroxenes >1500 ppm), high pyrope content in garnet (>34 mol.%), signs of metasomatism, and the absence of plagioclase can serve as objective criteria indicating the mantle origin of Grt-Cpx xenoliths.

Estimation of *P-T* parameters for xenoliths from the V.Grib pipe confirmed the mantle nature of eclogitic xenoliths (800-1200 °C, 30-50 kbar) and is consistent with the initial assumption of a lower crustal origin for granulitic xenoliths (750-800 °C, 14-15 kbar). Based on *P-T* parameters, Grt-granulites fall within the transitional domain between the eclogite facies and high-pressure granulites.

Since the problem of identifying lower crustal Grt-Cpx granulite xenoliths and mantle eclogites from the V.Grib pipe remains unresolved, it is proposed to conduct a comprehensive isotope-geochemical analysis of zircon already extracted by the authors from two lower crustal Grt-Cpx granulites, and to compare its isotope-geochemical characteristics with previously published data.

Access to data

Representative data on the composition of major and rare chemical elements in rock-forming and secondary minerals of mantle eclogites and garnet-clinopyroxene lower crustal granulites are available at the following links:

This is an open access article under the CC BY 4.0 license

Supplement 1, https://pmi.spmi.ru/pmi/article/download/16832/16630;
Supplement 2, https://pmi.spmi.ru/pmi/article/download/16832/16631;
Supplement 3, https://pmi.spmi.ru/pmi/article/download/16832/16632;
Supplement 4, https://pmi.spmi.ru/pmi/article/download/16832/16633.

The authors express their gratitude to O.L.Galankina (IPGG RAS), S.G.Simakin, and E.V.Potapov (Valiev IPT RAS, Yaroslavl Branch) for conducting the analytical work and thank the management of AGD Diamonds JSC for providing the rock material for research.

REFERENCES

1. Melnik A.E., Korolev N.M., Skublov S.G. et al. Zircon in mantle eclogite xenoliths: a review. *Geological Magazine*. 2021. Vol. 158. Iss. 8, p. 1371-1382. DOI: 10.1017/S0016756820001387
2. Brown M. Some thoughts about eclogites and related rocks. *European Journal of Mineralogy*. 2023. Vol. 35. Iss. 4, p. 523-547. DOI: 10.5194/ejm-35-523-2023
3. Aulbach S., Smart K.A. Petrogenesis and Geodynamic Significance of Xenolithic Eclogites. *Annual Review of Earth and Planetary Sciences*. 2023. Vol. 51, p. 521-549. DOI: 10.1146/annurev-earth-031621-112904
4. O'Brien P.J., Rötzler J. High-pressure granulites: formation, recovery of peak conditions and implications for tectonics. *Journal of Metamorphic Geology*. 2003. Vol. 21. Iss. 1, p. 3-20. DOI: 10.1046/j.1525-1314.2003.00420.x
5. Korikovsky S.P. Prograde transformations of gabbronorites during eclogitization in the temperature range 600-700 °C. *Russian Geology and Geophysics.* 2005. Vol. 46. N 12, p. 1333-1348.
6. Korikovsky S.P., Mirčovski V., Zakariadze G.S. Metamorphic evolution and the composition of the protolith of plagioclase-bearing eclogite-amphibolites of the Buchim Block of the Serbo-Macedonian Massif, Macedonia. *Petrology*. 1997. Vol. 5. N 6, p. 534-549.
7. Carswell D.A. Eclogites and the eclogite facies: definitions and classification. *Eclogite Facies Rocks*. Springer, 1990. P. 1-13.
8. Nikitina L.P., Ivanov M.V. Geological thermobarometry based on mineral-forming reactions involving phases of variable composition. St. Petersburg: Nedra, 1992, p. 162.
9. Skublov S.G., Petrov D.A., Galankina O.L. et al. Th-Rich Zircon from a Pegmatite Vein Hosted in the Wiborg Rapakivi Granite Massif. *Geosciences*. 2023. Vol. 13. Iss. 12. N 362. DOI: 10.3390/geosciences13120362
10. Rogova I.V., Stativko V.S., Petrov D.A., Skublov S.G. Trace Element Composition of Zircons from Rapakivi Granites of the Gubanov Intrusion, the Wiborg Massif, as a Reflection of the Fluid Saturation of the Melt. *Geochemistry International.* 2024. Vol. 62. N 11, p. 1123-1136. DOI: 10.1134/S0016702924700630
11. Skublov S.G., Nikitina L.P., Marin Yu.B. et al. U–Pb Age and Geochemistry of Zircons from Xenoliths of the V.Grib Kimberlitic Pipe, Arkhangelsk Diamond Province. *Doklady Earth Sciences.* 2012. Vol. 444. Part 1, p. 595-600. DOI: 10.1134/S1028334X12050066
12. Skublov S.G., Shchukina E.V., Guseva N.S. et al. Geochemical Characteristics of Zircons from Xenoliths in the V.Grib Kimberlite Pipe, Archangelsk Diamondiferous Province. *Geochemistry International.* 2011. Vol. 49. N 4, p. 415-421. DOI: 10.1134/S0016702911040082
13. Shchukina E.V., Agashev A.M., Golovin N.N., Pokhilenko N.P. Equigranular eclogites from the V. Grib kimberlite pipe: evidence of Paleoproterozoic subduction in the territory of the Arkhangelsk diamondiferous province. *Doklady Akademii nauk*. 2015. Vol. 462. N 2, p. 208-212. DOI: 10.7868/S0869565215140248
14. Heaman L.M., Creaser R.A., Cookenboo H.O., Chacko T. Multi-Stage Modification of the Northern Slave Mantle Lithosphere: Evidence from Zircon- and Diamond-Bearing Eclogite Xenoliths Entrained in Jericho Kimberlite, Canada. *Journal of Petrology*. 2006. Vol. 47. Iss. 4, p. 821-858. DOI: 10.1093/petrology/egi097
15. Shchukina E.V., Agashev A.M., Zedgenizov D.A. Origin of zircon-bearing mantle eclogites entrained in the V.Grib kimberlite (Arkhangelsk region, NW Russia): Evidence from mineral geochemistry and the U-Pb and Lu-Hf isotope compositions of zircon. *Mineralogy and Petrology*. 2018. Vol. 112. Suppl. 1, p. 85-100. DOI: 10.1007/s00710-018-0581-z
16. Nikitina L.P., Korolev N.M., Zinchenko V.N., Felix J.T. Eclogites from the upper mantle beneath the Kasai Craton (Western Africa): Petrography, whole-rock geochemistry and U-Pb zircon age. *Precambrian Research*. 2014. Vol. 249, p. 13-32. DOI: 10.1016/j.precamres.2014.04.014
17. Koreshkova M.Yu., Downes H., Glebovitsky V.A. et al. Zircon trace element characteristics and ages in granulite xenoliths: a key to understanding the age and origin of the lower crust, Arkhangelsk kimberlite province, Russia. *Contributions to Mineralogy and Petrology*. 2014. Vol. 167. Iss. 2. N 973. DOI: 10.1007/s00410-014-0973-y
18. Koreshkova M., Downes H., Millar I. et al. Geochronology of Metamorphic Events in the Lower Crust beneath NW Russia: a Xenolith Hf Isotope Study. *Journal of Petrology*. 2017. Vol. 58. Iss. 8, p. 1567-1590. DOI: 10.1093/petrology/egx065
19. Samsonov A.V., Nosova A.A., Tretyachenko V.V. et al. Collisional Sutures in the Early Precambrian Crust as a Factor Responsible for Localization of Diamondiferous Kimberlites in the Northern East European Platform. *Doklady Earth Sciences.* 2009. Vol. 425. N 2, p. 226-230. DOI: 10.1134/S1028334X09020111
20. Ustinov V.N., Neruchev S.S., Zagainyi A.K. et al. Diamonds in the North of the East-European Platform. St. Petersburg: Nauka, 2021, p. 410 (in Russian).
21. Vasilev E.A., Kriulina G.Yu., Garanin V.K. Spectroscopy of Diamonds from the M.V.Lomonosov Deposit. *Geology of Ore Deposits.* 2021. Vol. 63. N 7, p. 668-674. DOI: 10.1134/S1075701521070096

This is an open access article under the CC BY 4.0 license

22. Vasilev E.A., Kudriavtsev A.A., Klepikov I.V., Antonov A.V. Diversity of the Structure of Diamond Crystals and Aggregates: Electron Backscatter Diffraction Data. *Geology of Ore Deposits.* 2023. Vol. 65. N 7, p. 743-753. DOI: 10.1134/S1075701523070140

23. Pashkevich M.A., Alekseenko A.V. Reutilization Prospects of Diamond Clay Tailings at the Lomonosov Mine, Northwestern Russia. *Minerals*. 2020. Vol. 10. Iss. 6. N 517. DOI: 10.3390/min10060517

24. Vasilev E.A. Defects of diamond crystal structure as an indicator of crystallogenesis. *Journal of Mining Institute.* 2021. Vol. 250, p. 481-491. DOI: 10.31897/PMI.2021.4.1

25. Kozlov A.V., Vasilev E.A., Ivanov A.S. et al. Genetic geological model of diamond-bearing fluid magmatic system. *Journal of Mining Institute.* 2024. Vol. 269, p. 708-720.

26. Larionova Yu.O., Sazonova L.V., Lebedeva N.M. et al. Kimberlite Age in the Arkhangelsk Province, Russia: Isotopic Geochronologic Rb-Sr and $^{40}Ar/^{39}Ar$ and mineralogical data on phlogopite. *Petrology*. 2016. Vol. 24. N 6, p. 562-593. DOI: 10.1134/S0869591116040020

27. Serebryakov E.V., Gladkov A.S., Koshkarev D.A. Three-dimensional structural-material models of the formation of the Nyurbinskaya and Botuobinskaya kimberlite pipes (Yakutian Diamondiferous Province, Russia). *Geodynamics & Tectonophysics.* 2019. Vol. 10. N 4, p. 899-920 (in Russian). DOI: 10.5800/GT-2019-10-4-0448

28. Vasilev E.A., Ustinov V.N., Leshukov S.I. et al. Diamonds from V.Grib kimberlite pipe: Morphology and spectroscopic features. *Lithosphere.* 2023. Vol. 23. N 4, p. 549-563 (in Russian). DOI: 10.24930/1681-9004-2023-23-4-549-563

29. Garanin V.K., Garanin K.V., Vasilyeva E.P. et al. Mineralogy of mantle xenoliths from diamondiferous kimberlite pipe named after V.Grib (Arkhangelskaya diamondiferous province). Article 2. Gamet-clinopyroxene±ilmenitephlogopite±aggregates. *Izvestiya vysshikh uchebnykh zavedeniy. Geologiya i razvedka*. 2005. N 1, p. 23-29 (in Russian).

30. Dolivo-Dobrovolsky D.V. MINAL – a program for efficient work with chemical analyses of minerals. *Zapiski Rossiiskogo mineralogicheskogo obshchestva*. 2025. Vol. 154. N 1, p. 142-150 (in Russian). DOI: 10.31857/S0869605525010086

31. Krivovichev V.G., Gulbin Yu.L. Recommendations for mineral formula calculations from chemical analytical data. *Zapiski Rossiiskogo mineralogicheskogo obshchestva.* 2022. Vol. 151. N 1, p. 114-124 (in Russian). DOI: 10.31857/S0869605522010087

32. Locock A.J. An Excel spreadsheet to classify chemical analyses of amphiboles following the IMA 2012 recommendations. *Computers & Geosciences*. 2014. Vol. 62, p. 1-11. DOI: 10.1016/j.cageo.2013.09.011

33. Warr L.N. IMA–CNMNC approved mineral symbols. *Mineralogical Magazine*. 2021. Vol. 85. Iss. 3, p. 291-320. DOI: 10.1180/mgm.2021.43

34. McDonough W.F., Sun S.-s. The composition of the Earth. *Chemical Geology*. 1995. Vol. 120. Iss. 3-4, p. 223-253. DOI: 10.1016/0009-2541(94)00140-4

35. Ellis D.J., Green D.H. An experimental study of the effect of Ca upon garnet-clinopyroxene Fe-Mg exchange equilibria. *Contributions to Mineralogy and Petrology*. 1979. Vol. 71. Iss. 1, p. 13-22. DOI: 10.1007/BF00371878

36. Powell R. Regression diagnostics and robust regression in geothermometer/geobarometer calibration: the garnet-clinopyroxene geothermometer revisited. *Journal of Metamorphic Geology*. 1985. Vol. 3. Iss. 3, p. 231-243. DOI: 10.1111/j.1525-1314.1985.tb00319.x

37. Yang Ai. A revision of the garnet-clinopyroxene Fe^{2+}-Mg exchange geothermometer. *Contributions to Mineralogy and Petrology*. 1994. Vol. 115. Iss. 4, p. 467-473. DOI: 10.1007/BF00320979

38. Ravna K. The garnet–clinopyroxene Fe^{2+}-Mg geothermometer: an updated calibration. *Journal of Metamorphic Geology*. 2000. Vol. 18. Iss. 2, p. 211-219. DOI: 10.1046/j.1525-1314.2000.00247.x

39. Ashchepkov I.V., Rotman A.Y., Somov S.V. et al. Composition and thermal structure of the lithospheric mantle beneath kimberlite pipes from the Catoca cluster, Angola. *Tectonophysics*. 2012. Vol. 530-531, p. 128-151. DOI: 10.1016/j.tecto.2011.12.007

40. Beyer C., Frost D.J., Miyajima N. Experimental calibration of a garnet–clinopyroxene geobarometer for mantle eclogites. *Contributions to Mineralogy and Petrology*. 2015. Vol. 169. Iss. 2. N 18. DOI: 10.1007/s00410-015-1113-z

41. Newton R.C., Perkins III D. Thermodynamic calibration of geobarometers based on the assemblages garnet-plagioclase-orthopyroxene (clinopyroxene)-quartz. *American Mineralogist*. 1982. Vol. 67. N 3-4, p. 203-222.

42. Watson E.B., Wark D.A., Thomas J.B. Crystallization thermometers for zircon and rutile. *Contributions to Mineralogy and Petrology*. 2006. Vol. 151. Iss. 4, p. 413-433. DOI: 10.1007/s00410-006-0068-5

43. Smit K.V., Stachel T., Creaser R.A. et al. Origin of eclogite and pyroxenite xenoliths from the Victor kimberlite, Canada, and implications for Superior craton formation. *Geochimica et Cosmochimica Acta*. 2014. Vol. 125, p. 308-337. DOI: 10.1016/j.gca.2013.10.019

44. Aulbach S., Pearson N.J., O'Reilly S.Y., Doyle B.J. Origins of Xenolithic Eclogites and pyroxenites from the Central Slave Craton, Canada. *Journal of Petrology*. 2007. Vol. 48. Iss. 10, p. 1843-1873. DOI: 10.1093/petrology/egm041

45. Pernet-Fisher J.F., Howarth G.H., Yang Liu et al. Komsomolskaya diamondiferous eclogites: evidence for oceanic crustal protoliths. *Contributions to Mineralogy and Petrology*. 2014. Vol. 167. Iss. 3. N 981. DOI: 10.1007/s00410-014-0981-y

46. Rötzler J., Romer R.L., Budzinski H., Oberhänsli R. Ultrahigh-temperature high-pressure granulites from Tirschheim, Saxon Granulite Massif, Germany: P-T-t path and geotectonic implications. *European Journal of Mineralogy*. 2004. Vol. 16. N 6, p. 917-937. DOI: 10.1127/0935-1221/2004/0016-0917

47. Kryza R., Pin C., Vielzeuf D. High-pressure granulites from the Sudetes (south-west Poland): evidence of crustal subduction and collisional thickening in the Variscan Belt. *Journal of Metamorphic Geology*. 1996. Vol. 14. Iss. 4, p. 531-546. DOI: 10.1046/j.1525-1314.1996.03710.x

48. Taylor L.A., Neal C.R. Eclogites with Oceanic Crustal and Mantle Signatures from the Bellsbank Kimberlite, South Africa, Part I: Mineralogy, Petrography, and Whole Rock Chemistry. *The Journal of Geology*. 1989. Vol. 97. N 5, p. 551-567. DOI: 10.1086/629334

49. Morimoto N., Fabries J., Ferguson A.K. et al. Nomenclature of Pyroxenes. *Mineralogical Magazine*. 1988. Vol. 52. Iss. 367, p. 535-550. DOI: 10.1180/minmag.1988.052.367.15

50. Leake B.E., Woolley A.R., Arps C.E.S. et al. Nomenclature of Amphiboles: Report of the Subcommittee on Amphiboles of the International Mineralogical Association, Commission on New Minerals and Mineral Names. *Mineralogical Magazine*. 1997. Vol. 61. Iss. 405, p. 295-310. DOI: 10.1180/minmag.1997.061.405.13

51. Azimov P., Shtukenberg A. Numerical Modeling of Growth Zoning at Nonstationary Crystallization of Solid Solutions: Metamorphic Garnets. *Mathematical Geology*. 2003. Vol. 35. Iss. 4, p. 405-430. DOI: 10.1023/A:1024841907133

52. Lebedeva N.M., Nosova A.A., Sazonova L.V., Larionova Y.O. Metasomatized Xenoliths of Mantle Eclogites and Garnet Pyroxenites from the V.Grib Kimberlite, Arkhangelsk Province. *Petrology.* 2022. Vol. 30. N 5, p. 479-498. DOI: 10.1134/S0869591122050046

This is an open access article under the CC BY 4.0 license

53. Mikhailenko D., Golovin A., Korsakov A. et al. Metasomatic Evolution of Coesite-Bearing Diamondiferous Eclogite from the Udachnaya Kimberlite. *Minerals*. 2020. Vol. 10. Iss. 4. N 383. DOI: 10.3390/min10040383

54. Jacob D.E. Nature and origin of eclogite xenoliths from kimberlites. *Lithos*. 2004. Vol. 77. Iss. 1-4, p. 295-316. DOI: 10.1016/j.lithos.2004.03.038

55. Hacker B., Kylander-Clark A., Holder R. REE partitioning between monazite and garnet: Implications for petrochronology. *Journal of Metamorphic Geology*. 2019. Vol. 37. Iss. 2, p. 227-237. DOI: 10.1111/jmg.12458

56. Klein-BenDavid O., Pettke T., Kessel R. Chromium mobility in hydrous fluids at upper mantle conditions. *Lithos*. 2011. Vol. 125. Iss. 1-2, p. 122-130. DOI: 10.1016/j.lithos.2011.02.002

***Authors*: Ekaterina V. Stetskaya,** *Postgraduate Student* (*Empress Catherine II Saint Petersburg Mining University, Saint Petersburg, Russia*), *yekaterina.logunova.02@mail.ru, https://orcid.org/0009-0001-1547-8176*, **Laysan I. Salimgaraeva,** *Candidate of Geological and Mineralogical Sciences, Researcher* (*Institute of Precambrian Geology and Geochronology RAS, Saint Petersburg, Russia*), *https://orcid.org/0000-0002-3285-847X*, **Aleksei V. Berezin,** *Candidate of Geological and Mineralogical Sciences, Senior Researcher* (*Institute of Precambrian Geology and Geochronology RAS, Saint Petersburg, Russia*), *https://orcid.org/0000-0002-5324-5840*, **Viktor N. Ustinov,** *Doctor of Geological and Mineralogical Sciences, Advisor to the General Director (AGD Diamonds JSC, Arkhangelsk, Russia*), *https://orcid.org/0000-0002-6565-6575*, **Roman N. Pendelyak,** *Head of Department* (*AGD Diamonds JSC, Arkhangelsk, Russia*), *https://orcid.org/0009-0004-7798-2118*.

The authors declare no conflict of interests.

This is an open access article under the CC BY 4.0 license